A NEW PROPOSED SHEPHERD MODEL OF A LI-ION OPEN CIRCUIT BATTERY BASED ON DATA FITTING

Hanane Hemi, Nacer K M'Sirdi, Aziz Naamane

A NEW PROPOSED SHEPHERD MODEL OF A LI-ION OPEN CIRCUIT BATTERY BASED ON DATA FITTING

Hanane Hemi[(a)], **Nacer K M'Sirdi**[(b)], **Aziz Naamane**[(c)]

[(a)(b)(c)]Aix Marseille University, CNRS, LIS, SASV, Marseille, France

[(a)]hanane.hemi@uqtr.ca, [(b)]nacer.msirdi@lis-lab.fr, [(c)]ziz.naamane@lis-lab.fr

ABSTRACT

In this paper, the effect of environment parameters on the Lithium ion (Li-ion) battery behaviour is studied. In fact, the experimental database collected from a Lithium-ion battery is used to study its dynamic behaviour and then propose a dynamic battery model who can describe the relationship between the Open Circuit Voltage (*OCV*), the State Of Charge (*SOC*) and the ambient temperature (T_a). The proposed Shepherd model of a Li-ion open circuit battery voltage *OCV* is adjusted by using the experimental database of the CALCE battery group CALCE and then this model is implemented and simulated by using MATLAB/Simulink tools.

Keywords : Data fitting; Li-ion battery; LiFePO4; Open Circuit Voltage; State Of Charge; Electrical vehicle.

1. INTRODUCTION

Energy storage with the Lithium ion (Li-ion) batteries are nowadays more and more deployed in many applications such in e-mobility and stationary storage. The rechargeable Li-ion in the electrical or the hybrid vehicles (EV/HEV) represent 72 % of the total rechargeable Li-ion battery cell market's value in 2022 know-made.com (2017).

In fact, Li-ion batteries technology has a high power/energy density, with high cell voltage. In addition, it has a high life span, and a low self discharge rate Tian et al. (2017) Waldmann et al. (2018).

For Example, in hybrid and electrical vehicles application, a Li-ion battery pack is considered as a secondary source of power, and it used to support and to reduce the fuel consumption from the primary source of power. During a driving cycle, Li-ion battery can assist a primary source of power during acceleration and can be charged either per it or by recovering braking energy during deceleration. Then, it plays a significant role in the overall efficiency. It allows also to reduce the consumption of the primary power source (as for example, the consumption of a hydrogen in the case of a fuel cell vehicle, or the consumption of the conventional fuel in the case of the Hybrid electric-petroleum vehicles).

However, some environmental or conditions of operation can have a negative effect on its behavior (current, voltages and State of Charge) and also on its life span. The influence of environmental conditions like ambient and storage system temperatures are very important factors that can help to predict its life time decrease and to prevent the probability of its damage and thermal runaway. Therefore, a good knowledge of the system heating and the heat transfer by the battery cell and then the battery pack, becomes crucial.

To protect battery pack from these inconveniences. A Battery Management System (BMS) has to be added to the system. The BMS will indeed may avoid under-voltage / over-voltage, short-circuit and thermal runaway of the battery pack and the then system can operates in safe zone Castano et al. (2015).

Modeling the behaviour of a Li-ion battery becomes then paramount to study a battery performance, depending on several external or internal conditions. In another hand, a behaviour model is useful to estimate and predict the current and future battery state variables. Its use is also interesting to manage the control for a safe battery operation on the other.

In this part, we focus our study on the influence of ambient temperature on battery performance. In particular, the impact of temperature on battery open circuit voltage (*OCV*).

In fact, the ambient temperature has a significant impact on battery State Of charge (*SOC*). Then an estimation and / or a prediction of the battery *SOC* will be harder and then it will be harder too to know the optimal charge/discharge range to control of batteries. However, knowing that *OCV* and *SOC* are dependent on ambient temperature, it is important to model this dependence by studying data from experimental battery measurement.

This paper is structured in three sections and a conclusion.The section 2. describes the experimental data and Test Analysis. The section 3. presents and describes the Lithium Ion battery standard *OCV* model equations. The section 4. presents the Lithium Ion battery Proposed *OCV* Model. Section 5. presents the conclusions on our results.

2. EXPERIMENTAL DATA AND TEST ANALYSIS

In this paper, the A123 battery cell has been selected. This battery is a LiFePO4 battery and its database had been proposed by the CALCE battery group CALCE Xing et al. (2014). This choice of this type of battery is motivated by the fact that is typically used in HEV applications.

The objective of this section is to present a battery data. In fact, by managing and analyzing this data, the relationship between the *OCV*, *SOC* at different ambiant temperatures (T_a) can be shown. In order to ensure this, a low-current *OCV* method had been used and provided for this test.

In fact, the Low-current *OCV* test consist by using a small current to charge and discharge the battery and then measure the battery output voltage. In this test, this output voltage is approximately equal to the *OCV*. This test had been performed for different ambient temperature varying from $T_a = -10$ °C to $T_a = 50$ °C with interval of $\Delta T_a = 10$ °C.

For each temperature, in the first step, the battery had been discharged at a constant current rate of $C/20$ until the output voltage reach to the value of lower cut-off voltage of 2 V. Then, in the second step, the battery had been charge using a constant current until the out put voltage reached the upper cut-off voltage of 3.6 V. These characteristics are given by battery manufacturer for battery security operation. Tab.1 shows the battery characteristics given by battery manufacturer A123Systems.

Table 1: Battery characteristics given by battery manufacturer A123Systems

Type	LiFePO4	
Nominal capacity	1.1	Ah
Nominal voltage	3.3	V
Upper cut-off voltage	3.6	V
Lower cut-off voltage	2	V
Maximum continuous discharge current	30	A

Fig. 1 presents the test bench for battery tests experiments He et al. (2014). Test bench detail has given by References CALCE He et al. (2014).

Fig.2a and Fig.2b present the *OCV* vs time at the discharge and the charge modes. As shown, the battery takes a long time to charge and discharge caused by the nature of this test (the Low-current *OCV* test). Also, by comparing *OCV* curves at different ambient temperatures, the time taken to charge or discharge a battery and *OCV* value depends on temperature.

Fig.3a and Fig.3b present the *OCV* vs the Capacity at the discharge and the charge modes. As shown in figures before, ambient temperature has an impact on battery behavior. In fact, the relation between *OCV* and battery capacity in both charge and discharge modes, is affected by the temperature.

As shown, the *OCV* is different for each temperature. In fact, at $t = 0$ s, the value of V_{oc} is different according to

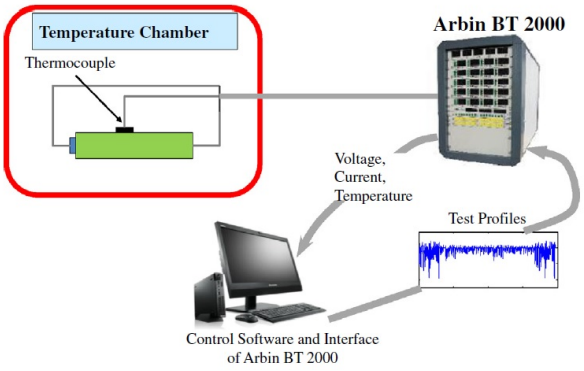

Figure 1: Test bench for battery tests experiments He et al. (2014)

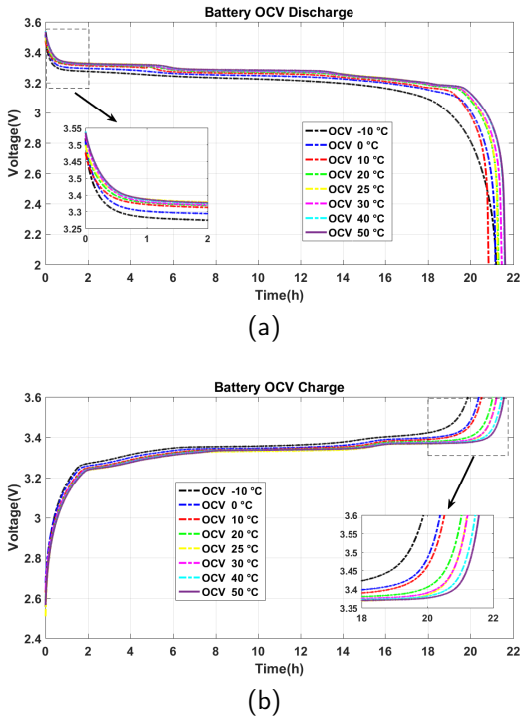

Figure 2: *OCV* vs time at discharge and Charge mode

temperature. In addition, the value of a couple $V_{oc} = 2$ V and battery capacity value at the lower cat-off voltage is affected. In fact, at 50 °C the discharge capacity value is higher comparing by lower temperatures. Also, for each *OCV* curve measured at ambient temperature, it is shown that is has some differences. By comparing the two temperature -10 °C and 50 °C, the battery behavior is affected and then *OCV* too.

3. LITHIUM ION BATTERY STANDARD *OCV* MODEL

Li-ion battery is considered as a part of the HEV system model. Therefore, to predict a HEV behavior in real time, a choice of a battery model is important for a real time

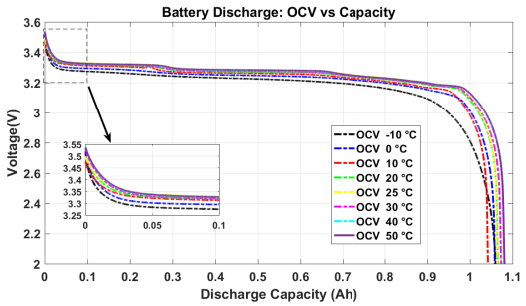

(a)

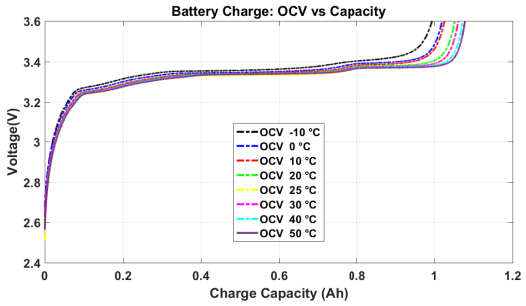

(b)

Figure 3: *OCV* vs Capacity at discharge and Charge mode

HEV operation, specially battery *SOC* for estimation and prediction BMS.

The Shepherd model consider the battery cell model composed by an internal resistance (R) and the open-circuit voltage (OCV). This model describes the mathematical relationship between voltage ($V_{Batt}(t)$), current ($i(t)$) for a constant current discharge. Eq.1 and Eq.2 represent this relationship Raszmann et al. (2017) Li and Ke (2011).

$$V_{Batt}(t) = V_0 - \frac{K.Q}{Q - i.t}.i(t) - R.i(t) \tag{1}$$

$$OCV(t) = V_0 - \frac{K.Q}{Q - i.t}.i(t) \tag{2}$$

where V_0 is the constant voltage (V), Q is the maximum capacity (Ah), $i.t$ is the discharged capacity (Ah), K is the polarization constant $(Ah)^{-1}$ and R is internal resistance. Fig.4 shows the ideal battery curve during discharge Raszmann et al. (2017). This figure shows that battery has tree zones. The fist one is the exponential zone. This zone presents an exponential curve of battery discharge which is described by two points: from the battery full charge (0,V_{full}) until the couple (Q_{exp},V_{exp}). The second zone is the nominal zone. this zone began from the end of exponential zone until the couple (Q_{nom},V_{nom}). This zone shows approximatively constant voltage. The latest zone is the full discharged battery zone. This zone began from the end of nominal zone until full battery discharge (Q_{full},0). This figure is important to find the battery parameters to be used in battery equation Eq.1. However, The Shepherd model equation does not include the exponential zone.

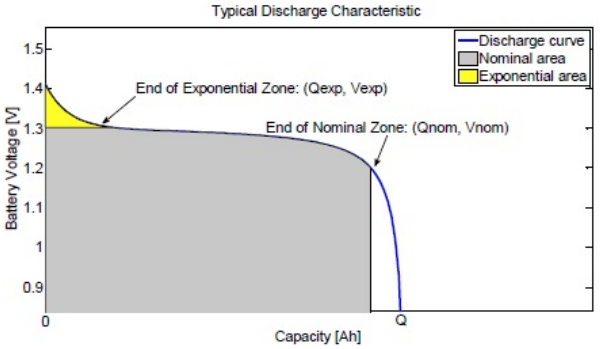

Figure 4: Ideal battery curve during discharge Gallo et al. (2013)

To improve a battery mathematical model to fit to battery charge and discharge curves, the Shepherd model had been modified by adding some terms. Eq.3 and Eq.4 show the *OCV* at discharge and charge modes respectively Raszmann et al. (2017) Gallo et al. (2013) Li and Ke (2011). If the current is positive, then the battery is in discharge mode, $V_{oc} = V_{oc.Discharge}$, as showed in Eq.3. If the current is negative, then the battery is in the charge mode, $V_{oc} = V_{oc.Charge}$, as presented in Eq.4. The *SOC* estimation has been given in Eq.5.

$$V_{oc.Discharge} = V_0 - \frac{K.Q}{Q - i.t}.i^* - \frac{K.Q}{Q - i.t}.i.t + A * e^{(-B.i.t)} \tag{3}$$

$$V_{oc.Charge} = V_0 - \frac{K.Q}{0.1 * Q - i.t}.i^* - \frac{K.Q}{Q - i.t}.i.t + A.e^{(-B.i.t)} \tag{4}$$

$$SOC = 1 - \frac{1}{Q}\int_0^t i(t).dt \tag{5}$$

$$A = V_{full} - V_{exp} \tag{6}$$

$$B = \frac{\alpha}{Q_{exp}} \tag{7}$$

$$K = \beta * [V_{full} - V_{nom} + A(e^{(-B\ Q_{nom})} - 1)] * \frac{Q_{full} - Q_{nom}}{Q_{nom}} \tag{8}$$

$$R = V_{nom} * \frac{1-\eta}{0.2 * Q_{nom}} \tag{9}$$

$$V_0 = V_{full} + K + R * i_{1C-rate} - A \tag{10}$$

where A is the exponential voltage (V) and also presents the amplitude of the exponential zone which is the difference between the voltage of battery fully charged and the end of the exponentiel voltage V_{exp} as shown in Eq.6 Raszmann et al. (2017).
B is the exponential capacity $(Ah)^{-1}$, or also called the time constant inverse Eq.7. This parameter is calculated from the charge capacity at the end of the exponentiel zone and also uses a constant value α. The α value is usually determined to improve the fit to a battery data Raszmann et al. (2017) Ahmed (2017).
K is the polarization constant $(Ah)^{-1}$ Raszmann et al. (2017), or also named polarizing voltage/resistance factor (V) Ahmed (2017) given in Eq.8. This parameter uses V_{full} value and also the end of nominal zone parameters (Q_{nom},V_{nom}). In Ref.Ahmed (2017), the constant β is added to improve the fit to a battery data.
V_0 is the constant voltage Eq.10. This parameter describe the battery voltage when a current is equal to zero Raszmann et al. (2017) Ahmed (2017).
R is the battery internal resistance (Ω) Eq.9. η is the efficiency of the battery and $i_{1C-rate}$ is the nominal current. i^* is the filtered current (A).
Generally, parameters of Eq.3 and Eq.4 are determined from battery datasheet provided by the battery manufacturer, especially from the curve of discharge at 1 C rate. However, those parameters depends on the variation of the temperature and the battery lifetime change. Therefore, The need to study and find the relation between those parameters and temperature is important.

4. LITHIUM ION BATTERY PROPOSED *OCV* MODEL

4.1. OCV Model parameter identification

The low-current test had been used on $LiFePO_4$ battery cell to identify the relationship between OCV - SOC and T_a. For each temperature T_a, the voltage and the SOC data are used to fit it with the Eq.3 by using data fitting, and then find parameters of this equation. Fig.5 presents a OCV fit and measured comparison for different temperatures. In this step, for each temperature, the parameters of the Eq.3 are founded by fitting the data to the curve. Then, seven equations for ambient temperature from $T_a = -10\,^{\circ}\text{C}$ to $T_a = 50\,^{\circ}\text{C}$ had been founded.
In addition, the Mean Absolute Error (MAE), the Root Mean Squared error (RMS) and the coefficient of determination or also named R-squared (R^2) are used to evaluate the efficiency of the fit as given in Eq.11, Eq.12 and Eq.13. The RMS error will be more sensitive to the variation of error than MAE due the fact that the calculation error is squared. In addition the R-squared will show how close the data measured are to the fitted regression curve. Then, the higher the R-squared, the better the model fits the measured voltage.

$$MAE = \frac{1}{n}\sum_{k=1}^{n} |V_{oc.measured,k} - V_{oc.calculated,k}| \tag{11}$$

$$RMS = \sqrt{\frac{1}{n}\sum_{k=1}^{n} (V_{oc.measured,k} - V_{oc.calculated,k})^2} \tag{12}$$

$$R^2 = 1 - \frac{SSR}{SSTot} \tag{13}$$

$$SSR = \sum_{k=1}^{n} (V_{oc.measured,k} - V_{oc.fit,k})^2 \tag{14}$$

$$SSTot = \sum_{k=1}^{n} (V_{oc.measured,k} - \overline{V_{oc.measured,k}})^2 \tag{15}$$

Where $(V_{oc.measured,k} - V_{oc.calculated,k})$ is the calculation error at time k. The model parameters and statistics are given in Tab.2. The Sum of Squared Error (SSR) is the quantity of how much the measurement points, vary around the estimated regression as shown in Eq.14. The sum of squared total (SSTot) is the quantity of how much the measurement points, vary around their mean as given in Eq.15.

Table 2: Model parameters and statistics for data fitting

T_a	MAE	RMS	R^2
-10 °C	0.0113	0.0093	0.9962
0 °C	0.0233	0.0128	0.9667
10 °C	0.0339	0.0161	0.9176
20 °C	0.0242	0.0140	0.9582
30 °C	0.0207	0.0132	0.9717
40 °C	0.0187	0.0137	0.9763
50 °C	0.0190	0.01344	0.9761

The next step is to study the relationship between those parameters and temperature. For each ambient temperature T_a, the following parameters A, B, K, V_0 are fitted. Fig.6 presents the exponential voltage (A) vs ambient temperature. The equation Eq.16 results from this fit have been chosen as a rational polynomials function. This function has a numerator polynomial and a denominator polynomial with a second degree. The degrees of the numerator and the denominator polynomial have been chosen to get the best curve fitting and minimum number of coefficients. The same approach has been used to find the other equations.
Eq.17 presents the exponential capacity (B) wich is chosen as a constant.

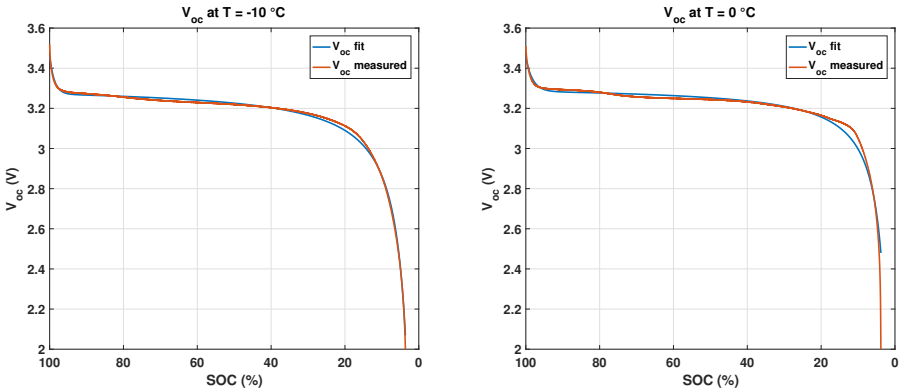

(a)

(b)

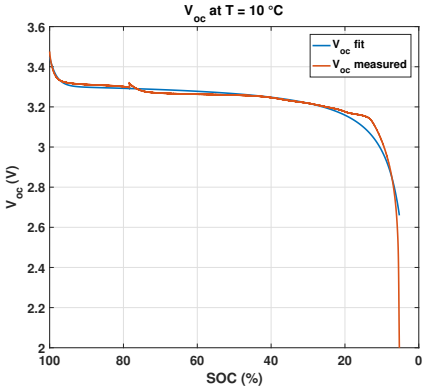

(c)

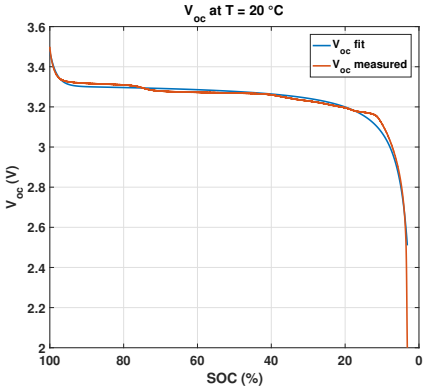

(d)

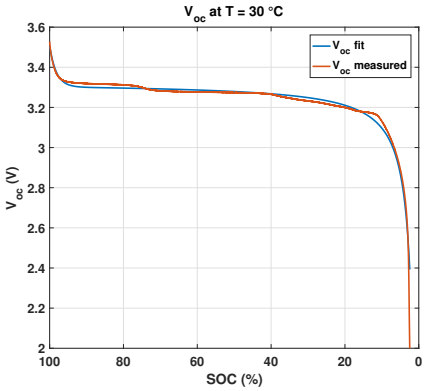

(e)

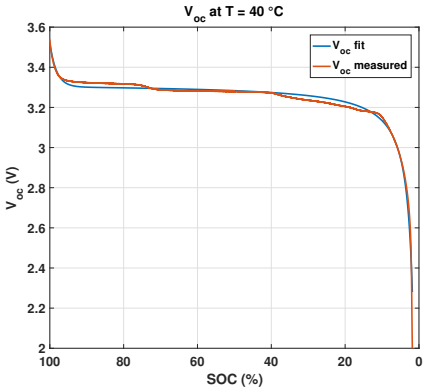

(f)

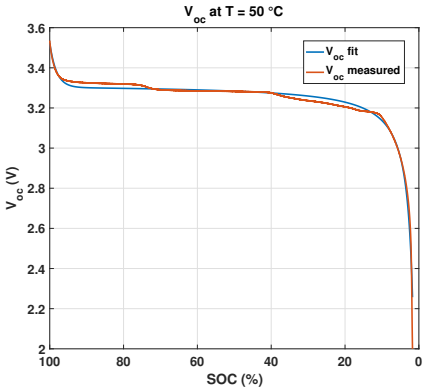

(g)

Figure 5: *OCV* fit and measured comparison for different temperatures

Fig.7 presents the polarization constant (K) vs temperature. This relationship Eq.18 is chosen as a rational polynomials function with a first degree in numerator polynomial and a denominator polynomial.
Fig.8 shows the constant voltage (V_0) vs temperature. This relationship Eq.19 is also chosen as a rational polynomials function. The numerator and denominator are a third and second degree polynomial respectively.

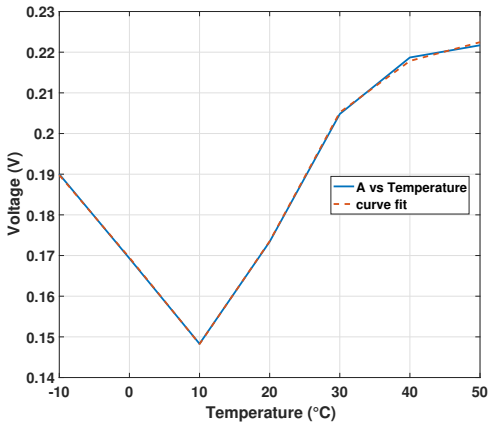

Figure 6: Exponential voltage A vs temperature

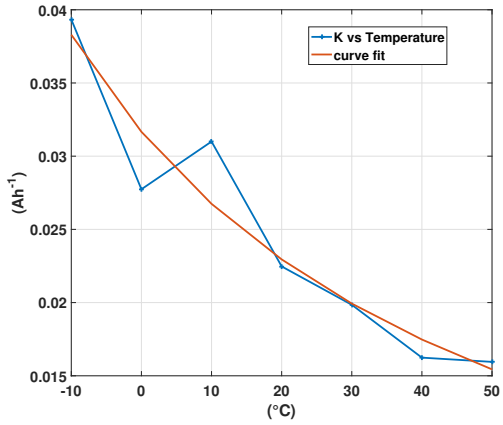

Figure 7: Polarization constant K vs temperature

$$A(T_a) = \frac{p_1\ T_a^2 + p_2\ T_a + p_3}{T_a^2 + q_1\ T_a + q_2} \tag{16}$$

$$B(T_a) = p_1 \tag{17}$$

$$K(T_a) = \frac{p_1\ T_a + p_2}{T_a + q_1} \tag{18}$$

$$V_0(T_a) = \frac{p_1\ T_a^3 + p_2\ T_a^2 + p_3\ T_a + p4}{T_a^2 + q_1\ T_a + q_2} \tag{19}$$

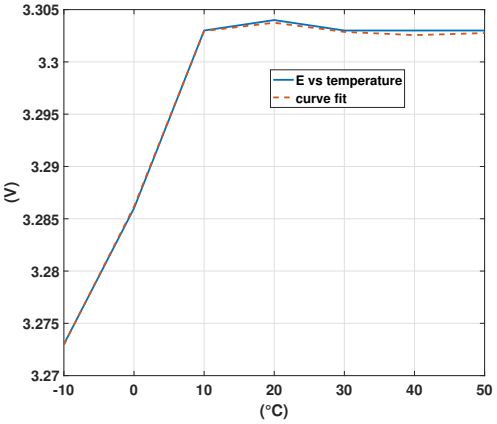

Figure 8: Constant voltage V_0 vs temperature

Table 3: Model parameters and statistics for A, K, and V_0

Parameters	MAE	RMS	R^2
A	0.00047	0.00037	0.9997
K	0.00229	0.00165	0.9167
V_0	0.00023	0.00019	0.9996

Those parameters performance resulting from fitting had been evaluated by using MAE, RMS and R^2 as shown in Tab.3.
The new equation of *OCV* is given in Eq.20. This equation highlights the relationship between the *OCV*, *SOC*, and T_a.

$$V_{oc.Discharge}(i.t, t, i^*, T_a) = V_0(T_a) - \frac{K(T_a).Q}{Q - i.t}.i^* - \frac{K(T_a).Q}{Q - i.t}.i.t + A(T_a) * e^{(-B.i.t)} \tag{20}$$

4.2. Validation of the proposed *OCV* model

The battery model shown in Fig.9 is used to simulate the proposed *OCV* model. In this case, the MATLAB/Simulink software and SimPowerSystems toolbox software packages is used for validation tests. As mentioned in section 2., the test used in this simulation is the Low-current *OCV* test. In fact, it consist by using a small current to charge and discharge the battery.
In this case, the current used to discharge a battery is equal to 0.05 A as shown in Fig.9a. Therefore, the output voltage measured is approximately equal to $V_{Batt} = V_{oc}$ as presented in Fig.9b. The *OCV* equation (Eq.20) is implemented as shown in the Fig.9c.
Fig.10 shows the *OCV* vs time measured and simulated comparison for different temperatures. In addition, Fig.11 shows the *OCV* vs *SOC* measured and simulated comparison for different temperatures.
The simulation results shows a small error between sim-

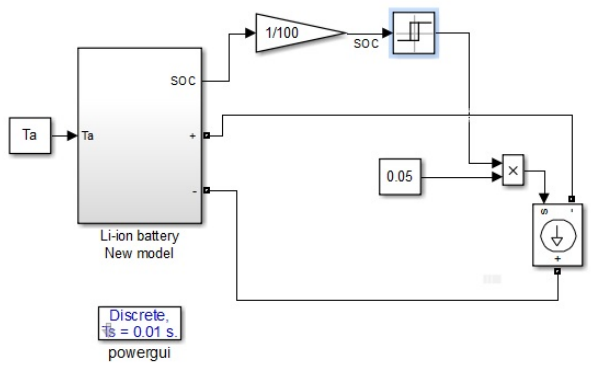

(a)

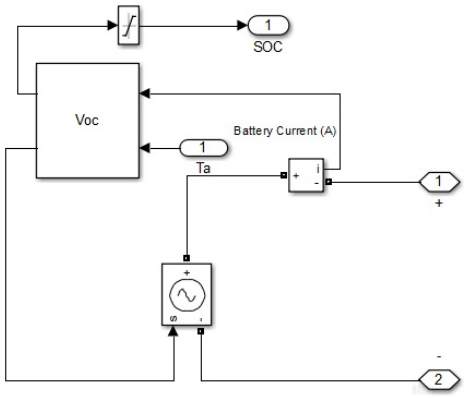

(b)

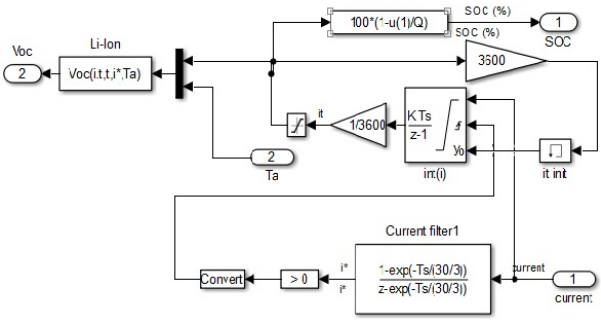

(c)

Figure 9: Battery model

ulations and measurements for ambient temperatures -10 °C, 20 °C, 30°C, 40°C, and 50 °C. However for ambient temperature 0 °C (Fig.10b and Fig.11b) and 10 °C (Fig.10c and Fig.11c), it is shown that the error is larger at the end of the discharge mode. Fig.10h and Fig.11h present *OCV* vs time and *OCV* vs *SOC* measured and simulated comparison respectively for all the ambient temperatures.

5. CONCLUSIONS

In this paper, we have proposed and compared the standard and the proposed *OCV* model. The first one is a Shepherd mathematical model modified and the second one is a proposed model based on a Shepherd mathematical model modified with the ambient temperature effect included to the model. The model has been fitted by using the experimental database of a LiFePO4 battery provided from the CALCE battery group CALCE. Also, the Low-current *OCV* test is used in this paper. In fact, this test consist to use a small current to charge and discharge the battery and then measure the battery output voltage. Therefore, the output voltage measured is approximately equal to $V_{Batt} = V_{oc}$.

The proposed model of a battery has been implemented and simulated by using MATLAB/Simulink tools.

The first step of this paper was to analyze a LiFePO4 database and find a relationship between *OCV*, *SOC* and ambient temperature T_a. In this case, a data fitting had been used to fit a data to a curve. In addition, MAE, RMS and R^2 have been used to evaluate the efficiency of the fit. In fact, the fit results presents a small error between the *OCV* fitted and measured for the different ambient temperatures from $T_a = -10$ °C to $T_a = 50$ °C.

The second step was to validate the proposed *OCV* model by simulation. Therefore, the simulation results have allowed to indicate small error between the *OCV* measured and simulated for the different ambient temperatures. However, for the ambient temperature 0 °C and 10 °C, the error is higher mostly in the end of the discharge mode.

In the next work, this model will be improved by reducing this error and also using other tests to study the complete battery system including the internal components.

ACKNOWLEDGMENT

The author would like to thank Professor Michael Pecht, from the CALCE battery group for sharing their experimental data and exchanges to let us use them for the model validation. “CALCE:Center for Advanced Life Cycle Engineering” https://web.calce.umd.edu/batteries/index.h

REFERENCES

A123Systems, (). A123 systems high power lithium ion apr18650m1a datasheet. https://www.batteryspace.com/prod-specs/6612.pdf.

Ahmed M., (2017). Modeling lithium-ion battery chargers in plecs®.

CALCE, (). Center for advanced life cycle engineering. https://web.calce.umd.edu/batteries/index.html.

Castano S., Gauchia L., Voncila E., and Sanz J., (2015). Dynamical modeling procedure of a li-ion battery pack suitable for real-time applications. Energy Conversion and Management, 92:396–405.

Gallo D., Landi C., Luiso M., and Morello R., (2013). Optimization of experimental model parameter identification for energy storage systems. Energies, 6 (9):4572–4590.

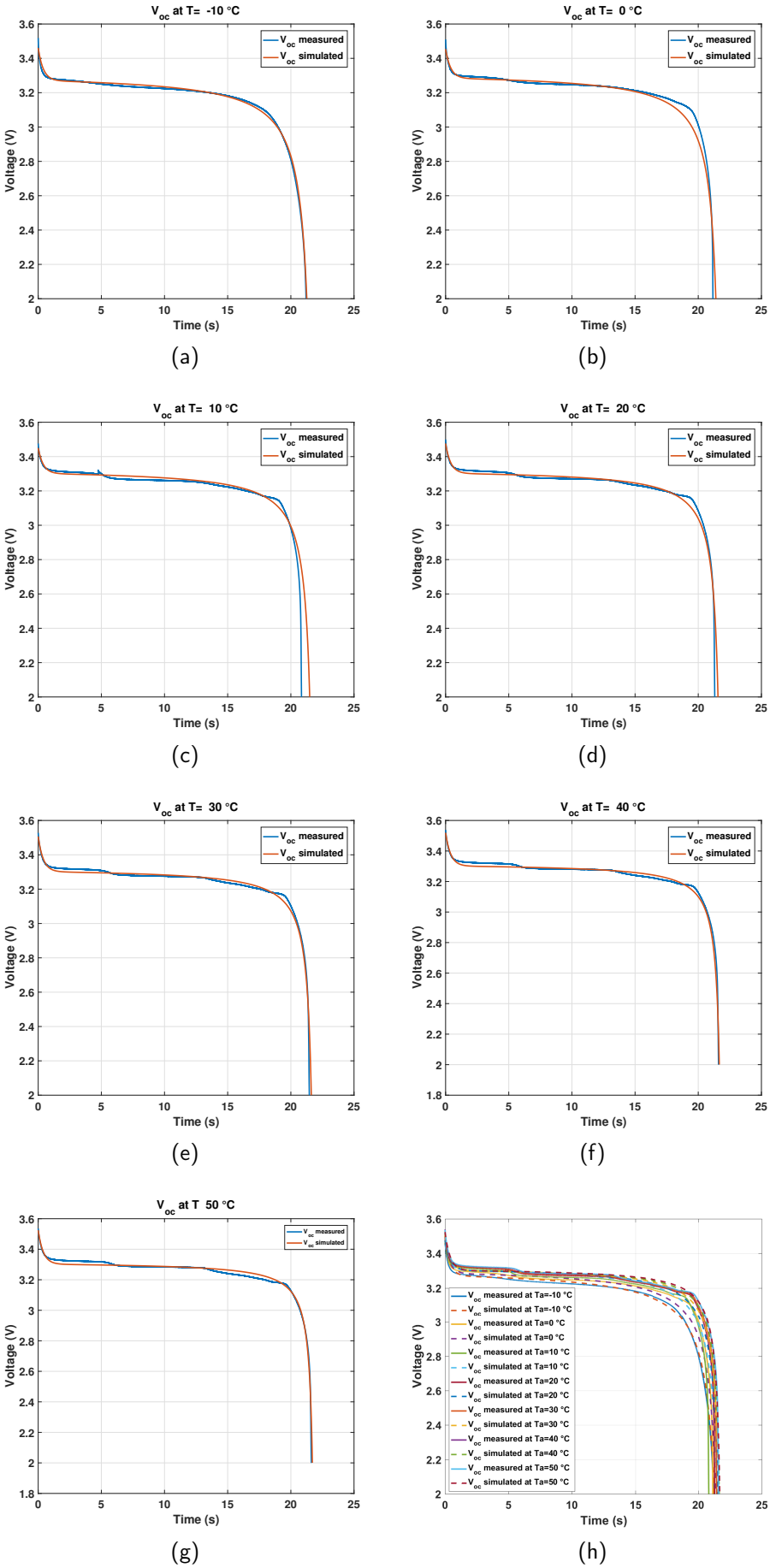

Figure 10: *OCV* vs time measured and simulated comparison for different temperatures

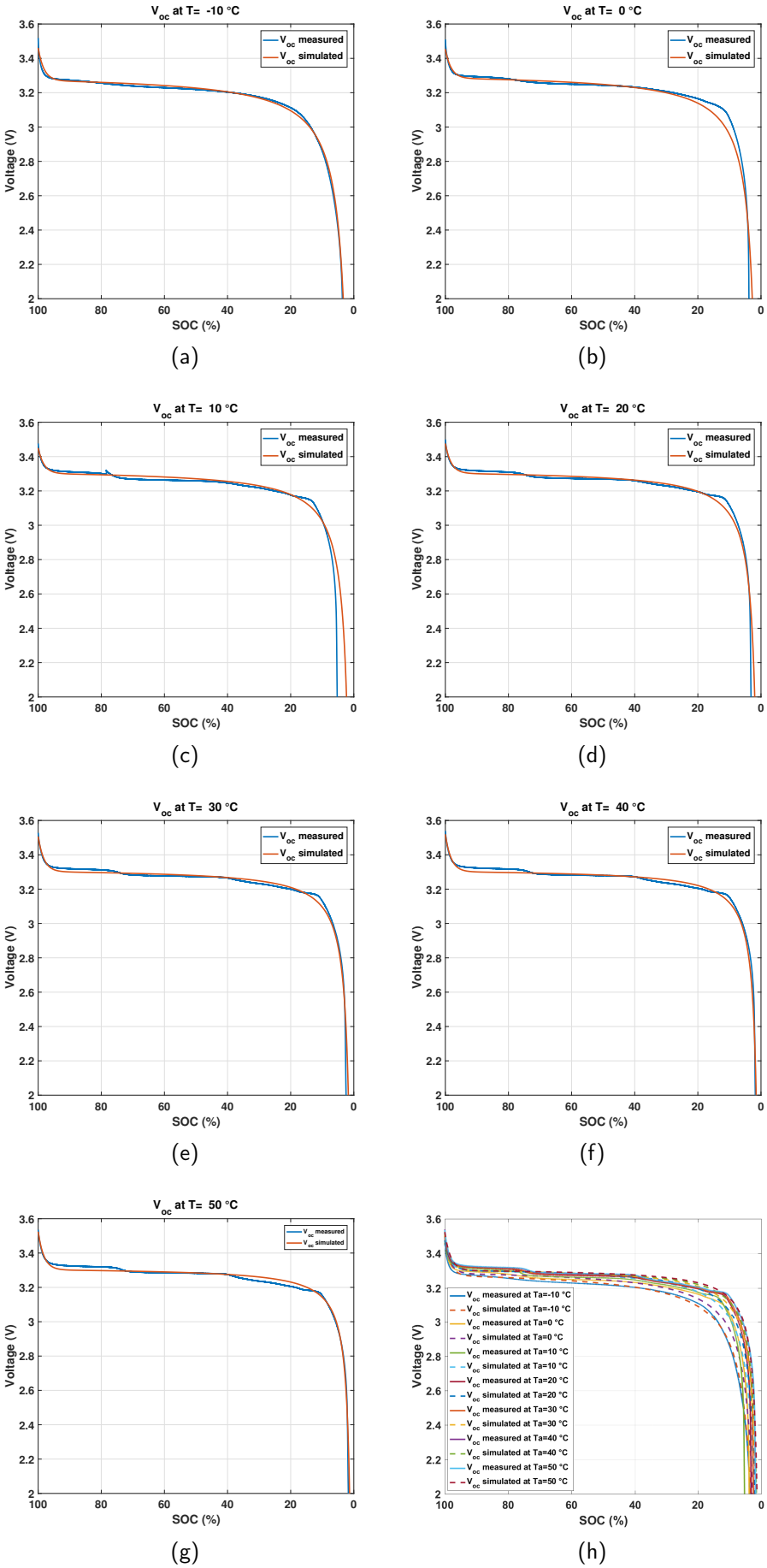

(a) (b) (c) (d) (e) (f) (g) (h)

Figure 11: *OCV* vs *SOC* measured and simulated comparison for different temperatures

He W., Williard N., Chen C., and Pecht M., (2014). State of charge estimation for li-ion batteries using neural network modeling and unscented kalman filter-based error cancellation. International Journal of Electrical Power & Energy Systems, 62:783–791.

knowmade.com, (2017). e-mobility: the new eldorado for li-ion batteries. https://www.knowmade.com/e-mobility-new-eldorado-li-ion-batteries/.

Li S. and Ke B., (2011). Study of battery modeling using mathematical and circuit oriented approaches. In: Power and Energy Society General Meeting, 2011 IEEE, IEEE, 1–8.

Raszmann E., Baker K., Shi Y., and Christensen D., (2017). Modeling stationary lithium-ion batteries for optimization and predictive control. In: Proceedings of the 2017 IEEE Power and Energy Conference at Illinois (PECI), Champaign, IL, USA, 23–24.

Tian Y., Li D., Tian J., and Xia B., (2017). State of charge estimation of lithium-ion batteries using an optimal adaptive gain nonlinear observer. Electrochimica Acta, 225:225–234.

Waldmann T., Hogg B.I., and Wohlfahrt-Mehrens M., (2018). Li plating as unwanted side reaction in commercial li-ion cells–a review. Journal of Power Sources, 384:107–124.

Xing Y., He W., Pecht M., and Tsui K.L., (2014). State of charge estimation of lithium-ion batteries using the open-circuit voltage at various ambient temperatures. Applied Energy, 113:106–115.